Supporting Information

Symmetry Breaking-Induced Double-Strand Helix in H-Bonded Coassembly

Juncong Liang,† Junhui Liang,‡ Aiyou Hao† and Pengyao Xing†*

†*Key Laboratory of Colloid and Interface Chemistry of Ministry of Education and School of Chemistry and Chemical Engineering, Shandong University, Jinan 250100, People's Republic of China. Email: xingpengyao@sdu.edu.cn*

‡*Department of Obstetrics and Gynecology, Shandong Provincial Hospital, Cheeloo College of Medicine, Shandong University, Jinan, 250021 People's Republic of China.*

Experimental section

Materials

All other starting chemicals and solvents were purchased from Aladdin Medicine Reagent Co. Ltd. and used without any further purification. **A7** was synthesized according to the ref. S1. Melamine derivates were synthesized according to the ref. S2. All water used in this work was deionized (DI) water.

Characterizations

Scanning electron microscope (SEM) images were attained by a Zeiss scanning electron microscope. The samples for SEM detection were dropped in the silicon pellet, dried and then sprayed by the gold. Transmission electron microscope (TEM) images were measured on a JEM-100CX II electron microscope. The samples for TEM detection were dropped in the copper grid and air-dried. X-ray diffraction (XRD) patterns were collected on a Rigaku SmartLab 9KW with Cu K_α radiation (λ= 0.15406 nm, voltage 40 KV, current 40 mA). The samples were casted onto cover glasses (18 mm × 18 mm) and dried to form thin film. CD were collected with an Applied Photophysics ChirascanV100 model. FT-IR was characterized on a Bruker

ALPHA model, and KBr was used as the disperse media. Single crystal data were collected on a Rigaku XtaLAB Synergy. X-ray diffraction (XRD) patterns were recorded on a PANalytical X□pert3 power diffractometer (40 kV, 40 mA) using Cu Ka radiation (λ= 0.15418 nm). It should be noted that the whole measurement was divided into two parts comprising small angle (0.5–10 degree) and wide angle (10–50 degree) regions. For XRD, assembled systems were centrifuged to remove solvents and non-assembled species, and the obtained aggregates were spread evenly on glass slide and air-dried at room temperature.

Assembly method

Amino acid derivatives and melamine derivatives were respectively dissolved in DMSO as concentrated stock solutions (100 mM). In order to trigger the co-assembly, a certain amount of stock solutions was mixed together, followed by the addition of DI water. Taking the preparation of **Fmoc-Gly**/**BaMm** co-assembly as an example. **Fmoc-Gly** and **BaMm** were dissolved in DMSO separately to obtain the stock solutions (100 mM). Then, **Fmoc-Gly** stock solution (30 μL) and **BaMm** stock solution (10 μL) were taken out by pipettes into a 1 mL vial, followed by gentle shaking to mix homogeneously. DI water (960 μL) was added by a pipette into the stock solution mixture. The vial was sealed by a cap and parafilm, and slightly shaken to make a homogenous phase (**Fmoc-Gly**: **BaMm** = 3 mM : 1 mM). An aging period at least for 8 h at room temperature was applied.

MD simulation

The geometries of **Fmoc-Gly** and **BaMm** were optimized by Gaussian View06 program, which were initially optimized, and the electrostatic potential (ESP) was simultaneously calculated by Hartree–Fork method at the B3LYP/6-31G (d) basis. The Antechamber program was used to fit the restrained electrostatic potential (RESP) charge, and then the general Amber force field (GAFF) was adopted to parameterize the for subsequent MD simulations. MD was performed using GROMACS and the details as following. The initial configuration was obtained by equilibration of SPC water in a triclinic simulation box with a length (x), width (y) and height (z) of 10, 10, 50 nm, respectively. Then, a cylindrical cavity with 3 nm radius was carved in the

center of the simulation box along the z axis. The molecules of 600 **Fmoc-Gly** and 200 **BaMm** with a length of 45 nm were placed randomly inside the cavity using PACKMOL. The MD simulations of **Fmoc-Gly**/**BaMm** coassembly system were carried out for 50 ns with a time step of 0.001 ps per integration step under the ensemble conditions of T = 298 K and 1 bar.

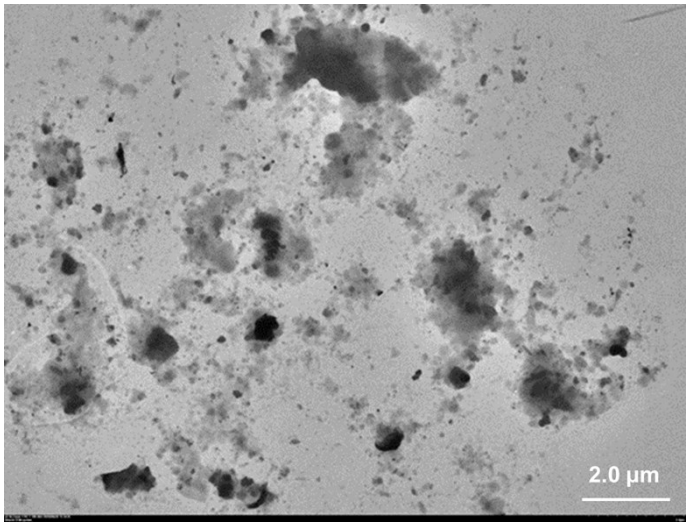

Figure S1. TEM image of **BnMm** self-assembly (3 mM).

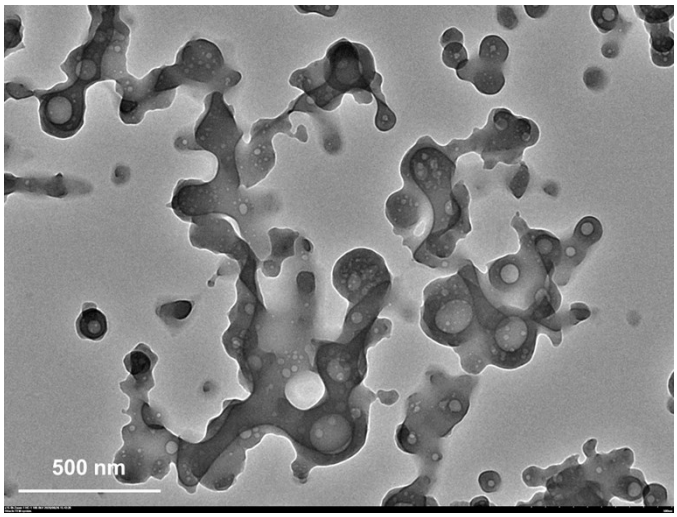

Figure S2. TEM image of **NaMm** self-assembly (3 mM).

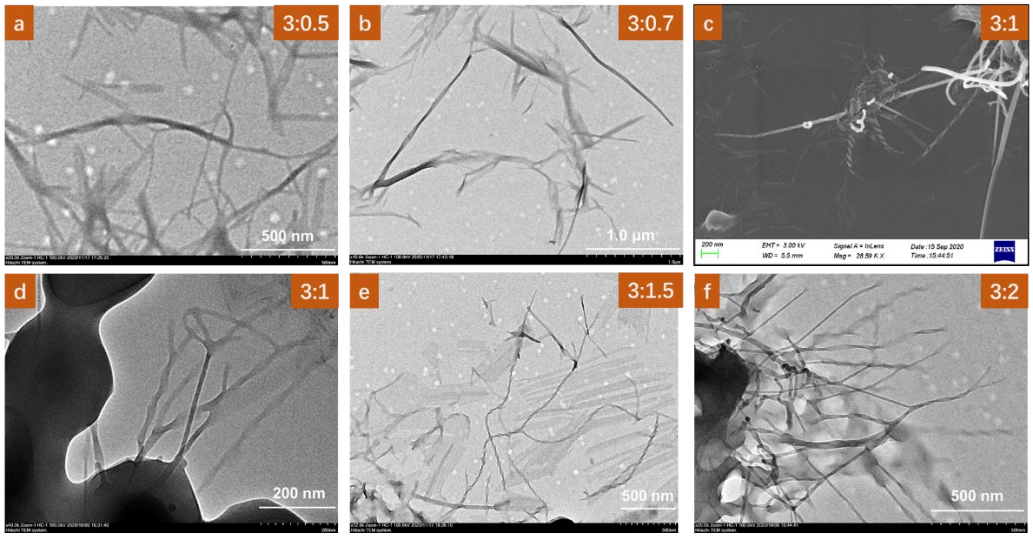

Figure S3. TEM (a,b, d-f) and SEM (c) images of **Fmoc-Gly**/**BaMm** co-assembly under different ratios. The ratios marked stand for the mM : mM.

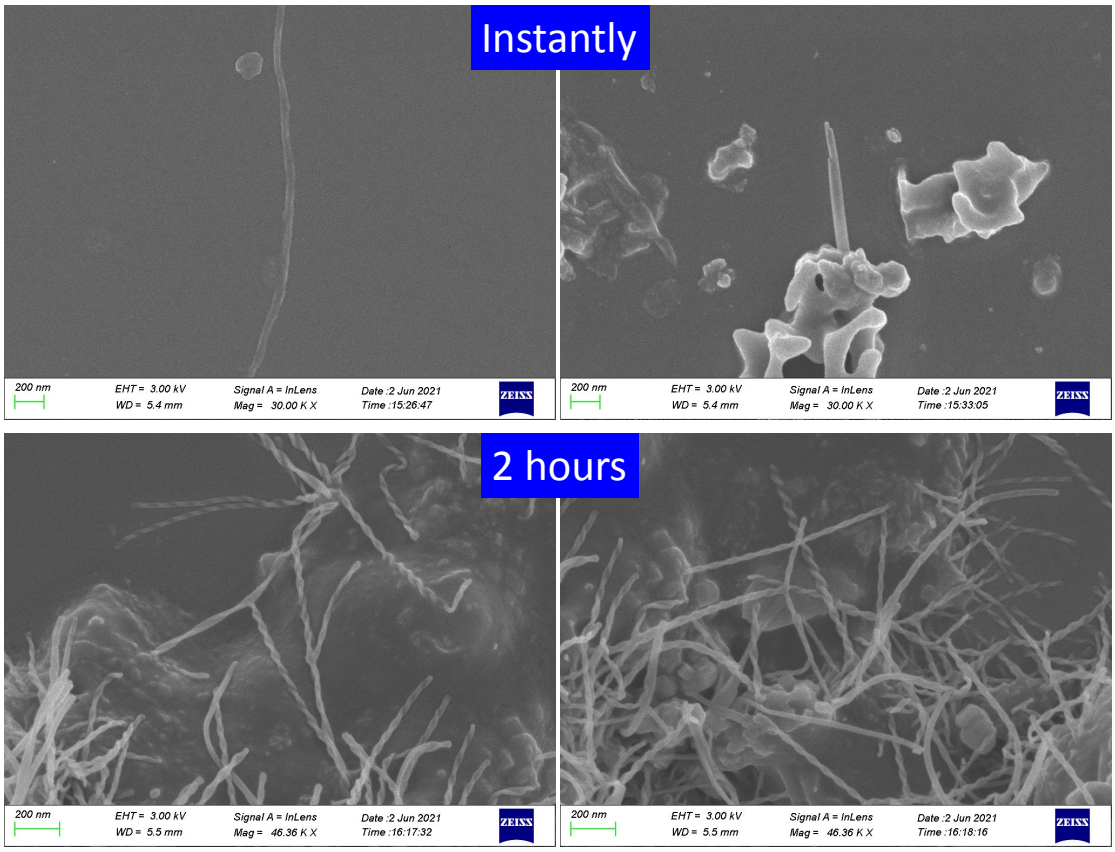

Figure S4. SEM (c) images of **Fmoc-Gly**/**BaMm** co-assembly (3:2) with different incubation time.

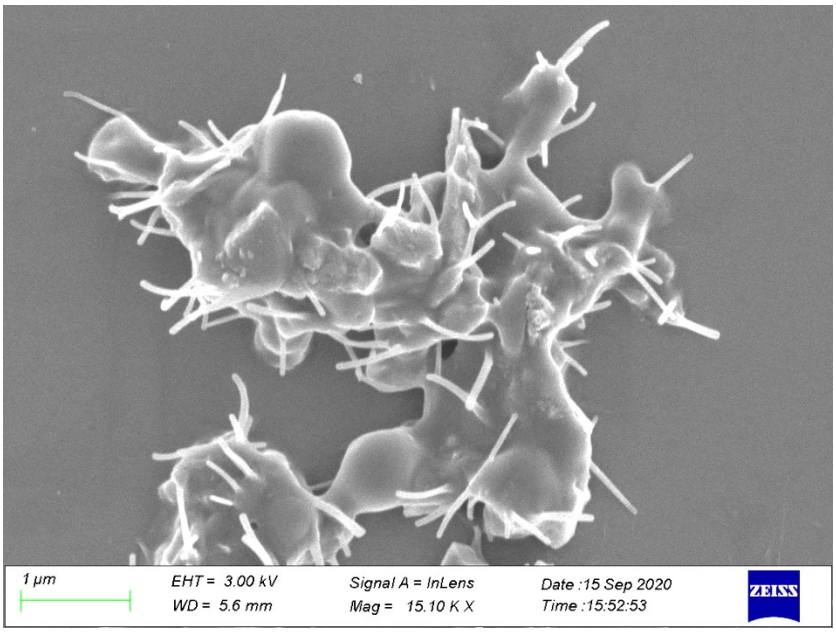

Figure S5 SEM image of co-assembled **Fmoc-Gly**/**BnMm** with the ratio 3 : 1 (mM).

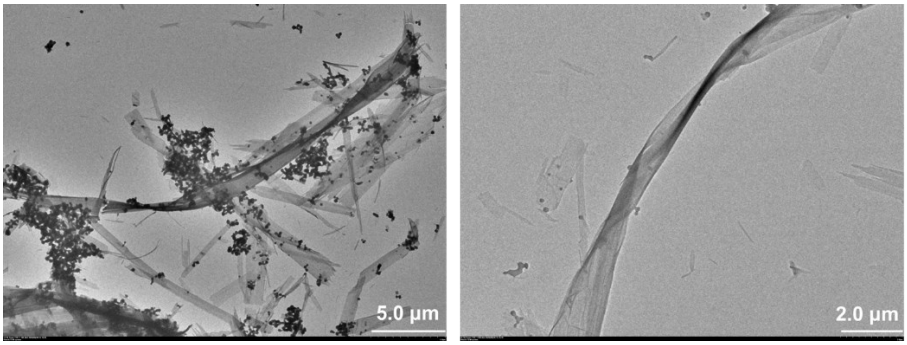

Figure S6 TEM images of co-assembled **Fmoc-Gly**/**NaMm** with the ratio 3 : 1 (mM).

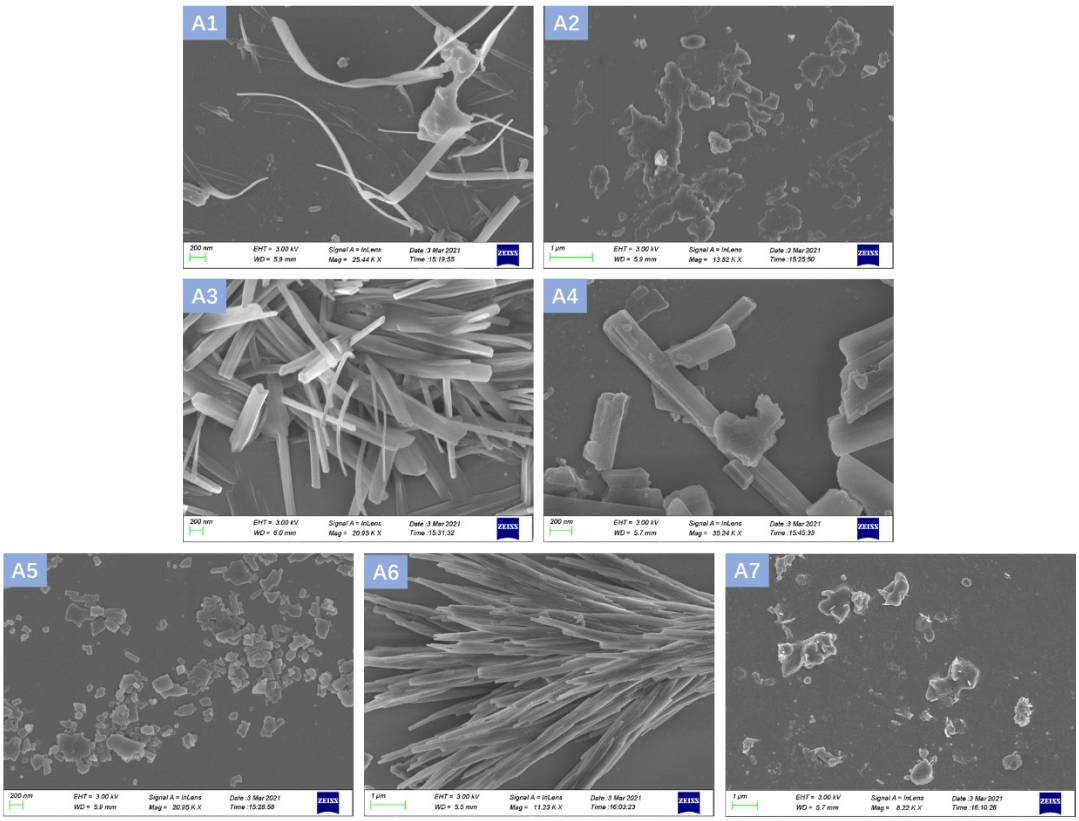

Figure S7 SEM images of co-assembled of **A1-A7** with **BaMm** with the ratio 3 : 1 (mM).

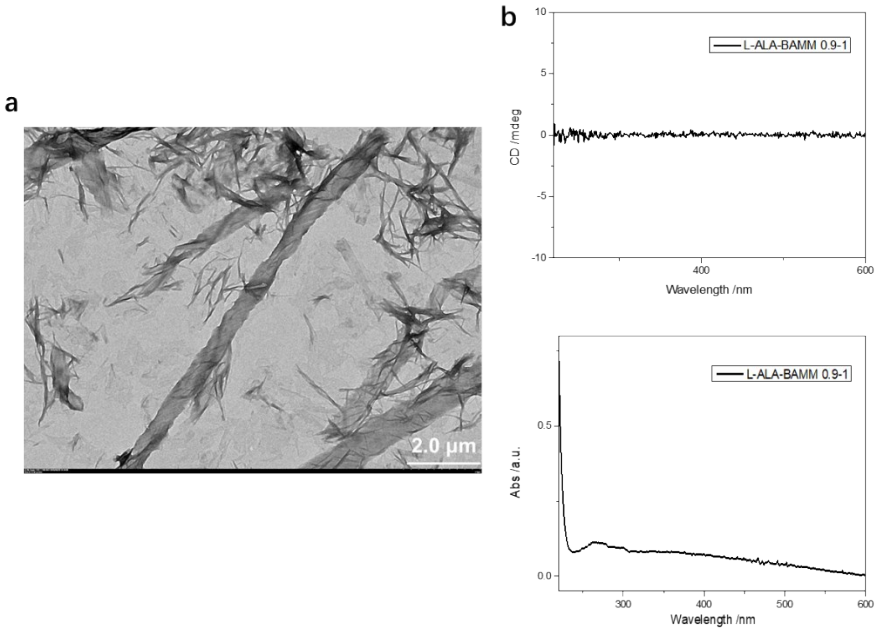

Figure S8 (a) TEM image of co-assembled *L*-**Ala/BaMm** with the ratio 3 : 1. (b) CD and corresponding UV-vis spectrum.

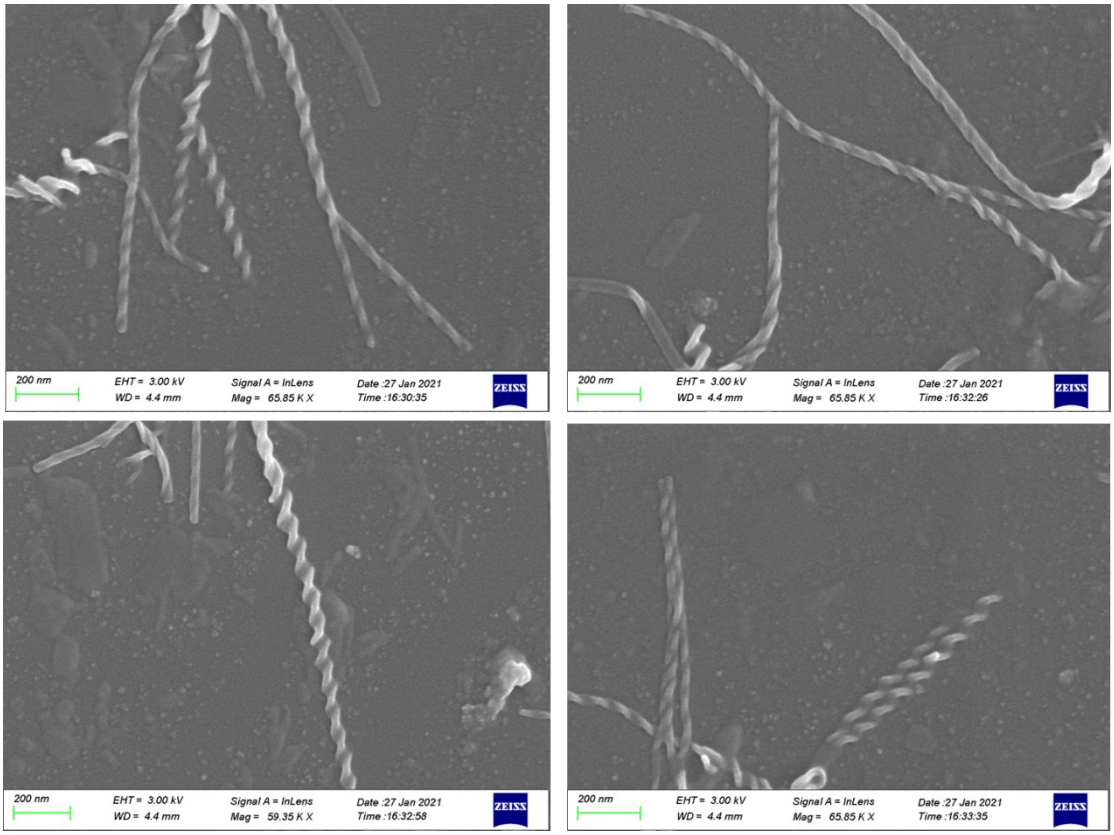

Figure S9. SEM images of *L*-**Ala/Fmoc-Gly/BaMm** coassemblies (0.3 : 3 : 1 mM).

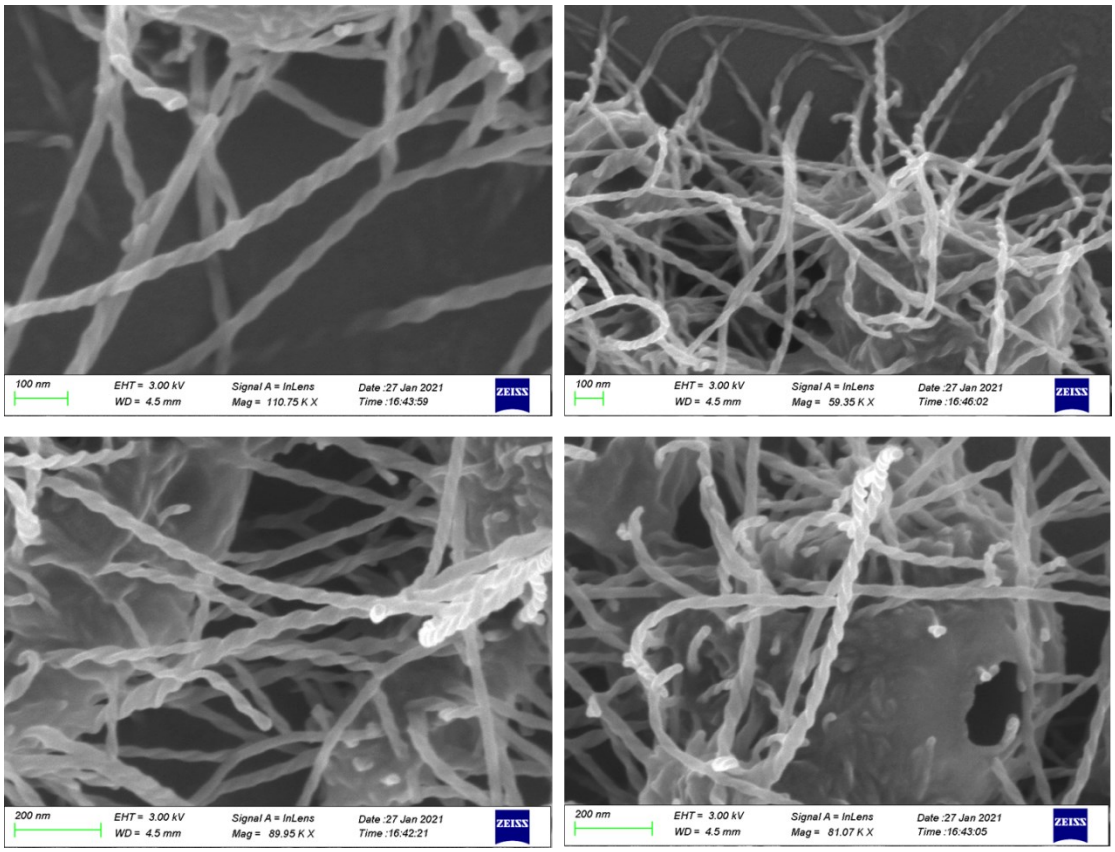

Figure S10. SEM images of *D*-**Ala/Fmoc-Gly/BaMm** coassemblies (0.3 : 3 : 1 mM).

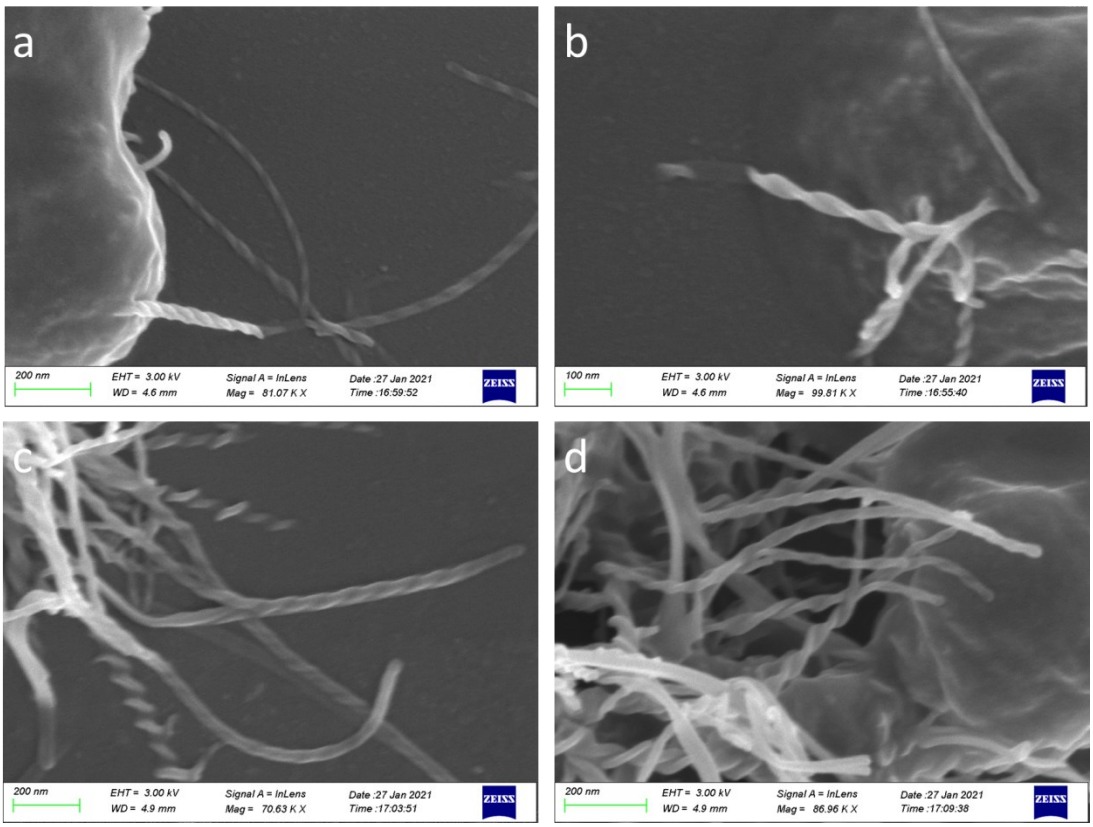

Figure S11. a,b) SEM images of *L*-**Ala/Fmoc-Gly/BaMm** coassemblies (0.3 : 3 : 1.5 mM); c,d) SEM images of *D*-**Ala/Fmoc-Gly/BaMm** coassemblies (0.3 : 3 : 1.5 mM).

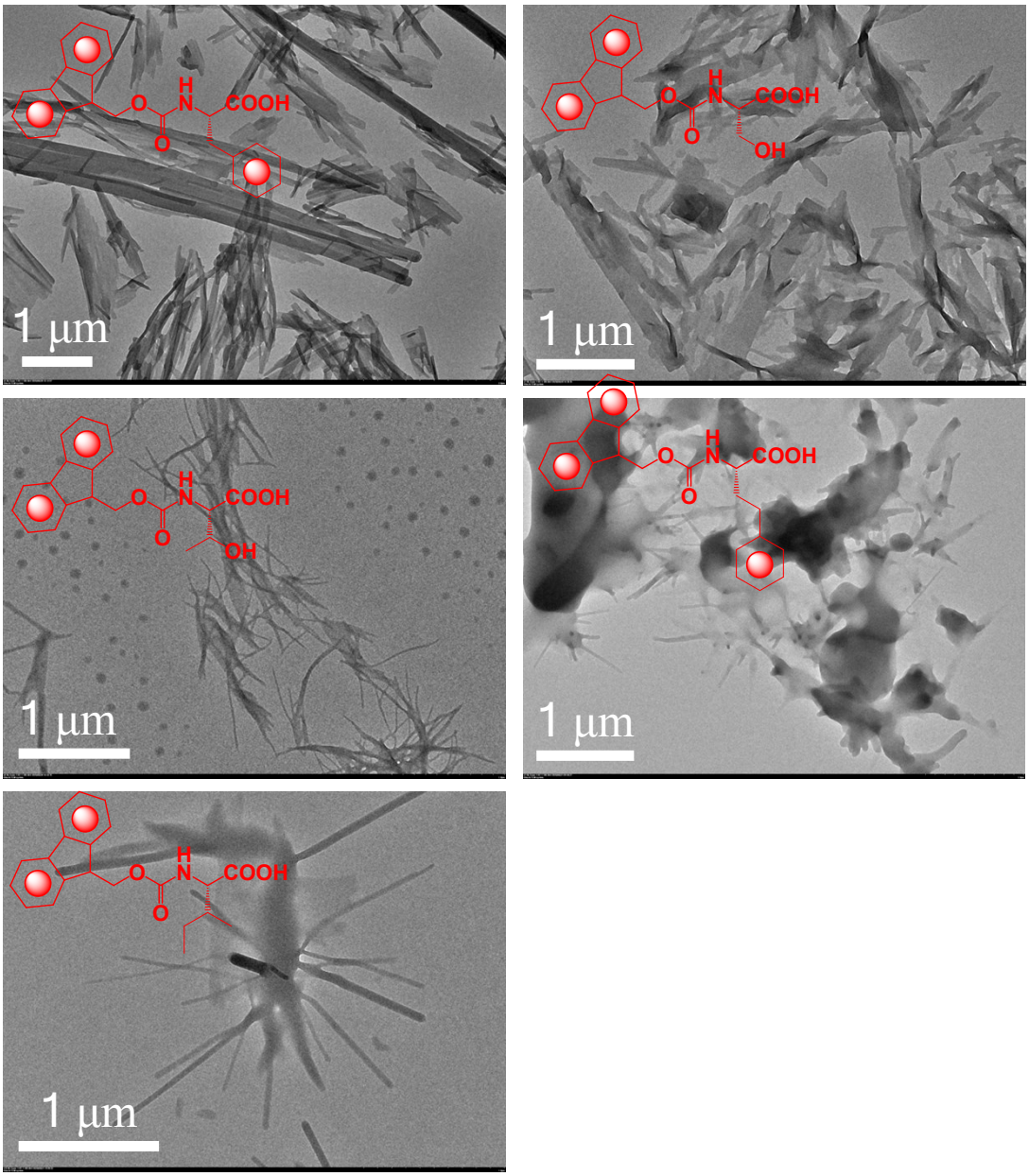

Figure S12. TEM images of binary coassemblies of several Fmoc-amino acaids with BaMm (3:1 by molar).

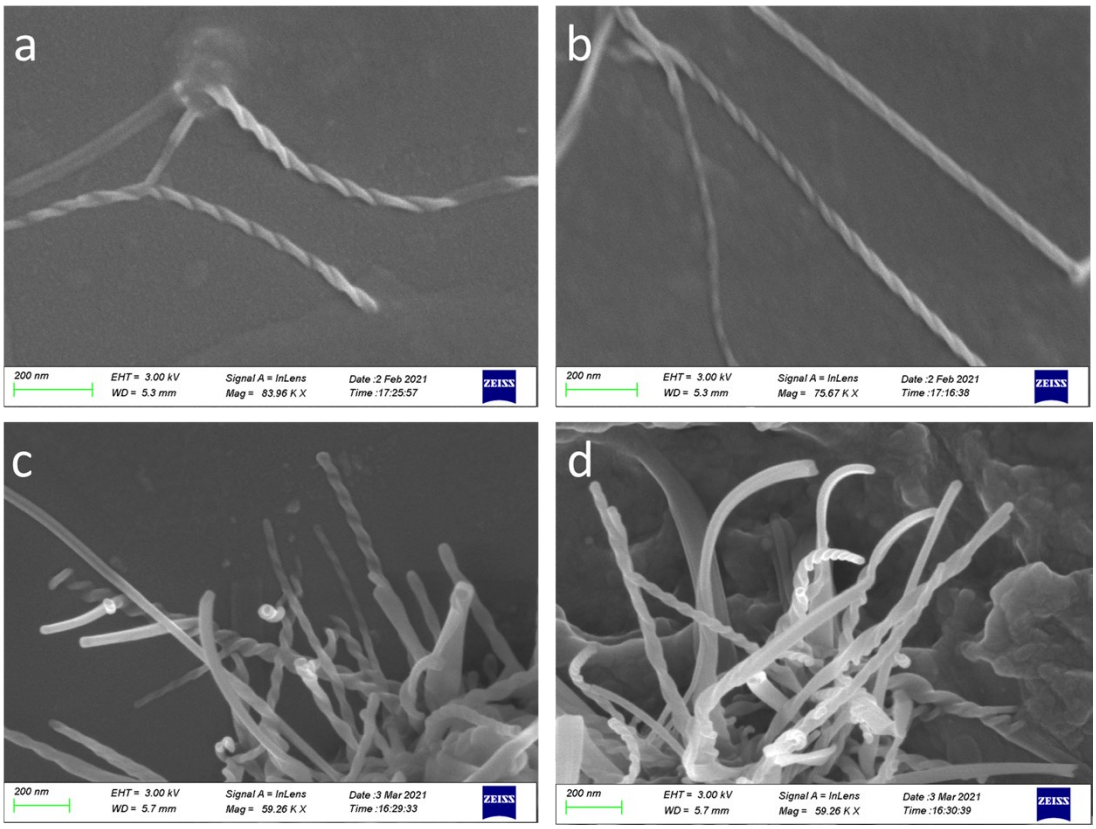

Figure S13. a,b) SEM images of *L*-**Asp/Fmoc-Gly/BaMm** coassemblies (0.3 : 3 : 1 mM); c,d) SEM images of *D*-**Asp/Fmoc-Gly/BaMm** coassemblies (0.3 : 3 : 1 mM).

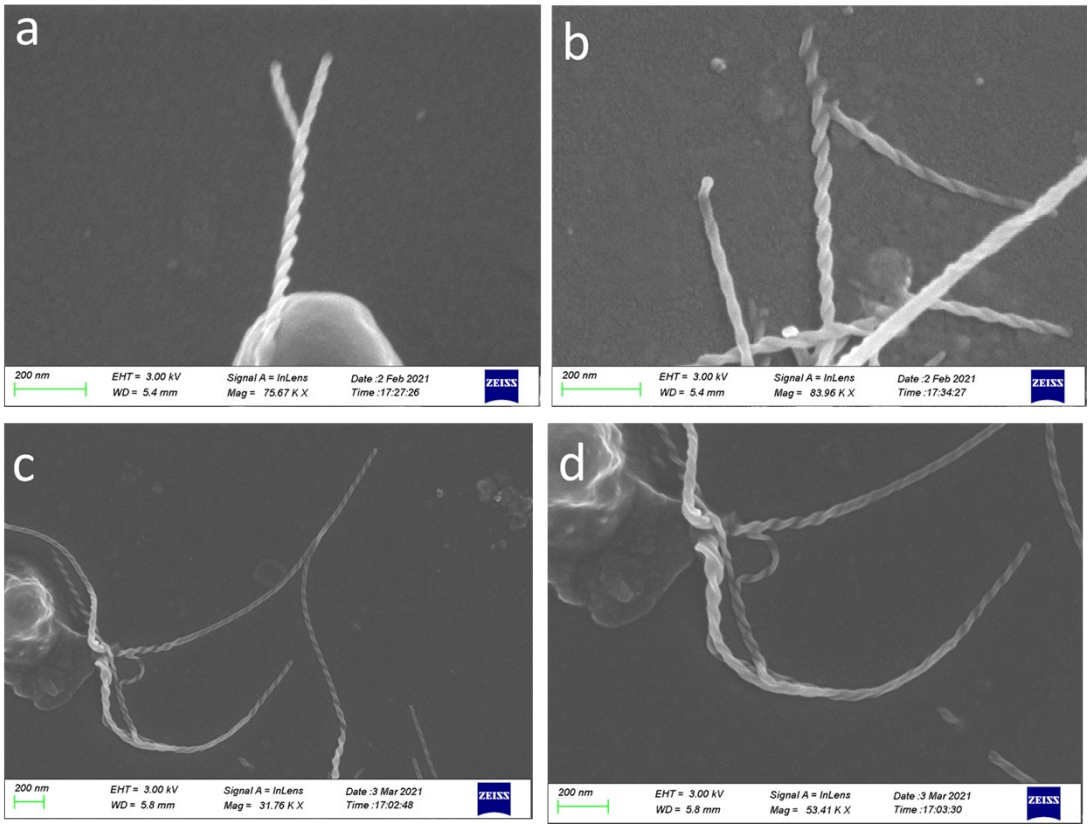

Figure S14. a,b) SEM images of *L*-**Phe/Fmoc-Gly/BaMm** coassemblies (0.3 : 3 : 1 mM); c,d) SEM images of *D*-**Phe/Fmoc-Gly/BaMm** coassemblies (0.3 : 3 : 1 mM).

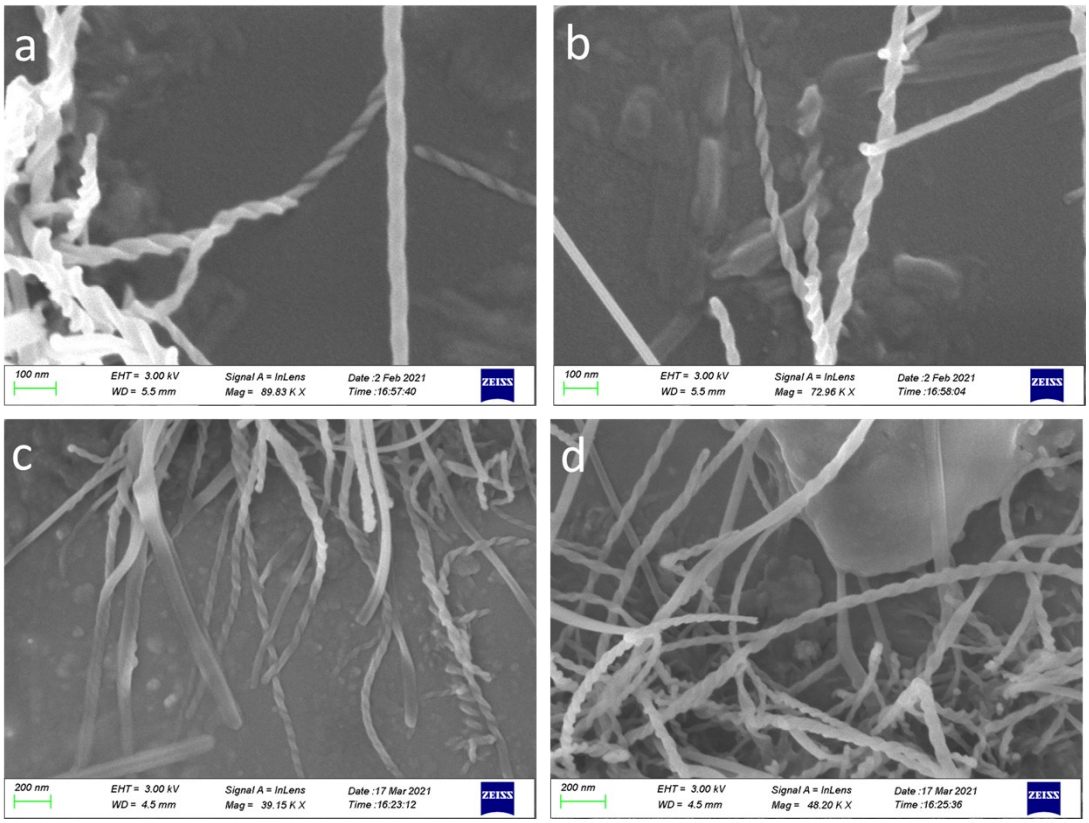

Figure S15. a,b) SEM images of *L*-**Ser/Fmoc-Gly/BaMm** coassemblies (0.3 : 3 : 1 mM); c,d) SEM images of *D*-**Ser/Fmoc-Gly/BaMm** coassemblies (0.3 : 3 : 1 mM).

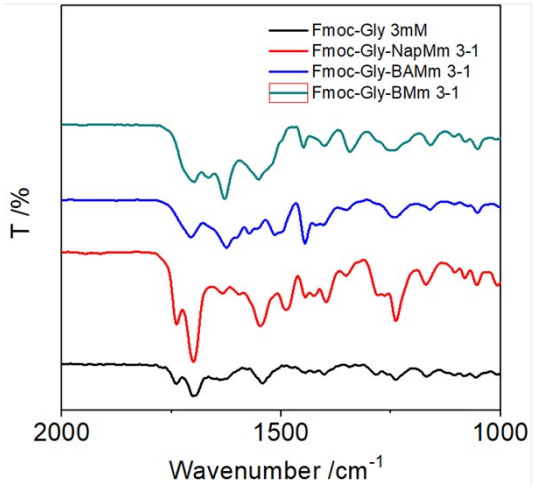

Figure S16 FT-IR spectra of co-assembly of **Fmoc-Gly** with melamine derivatives.

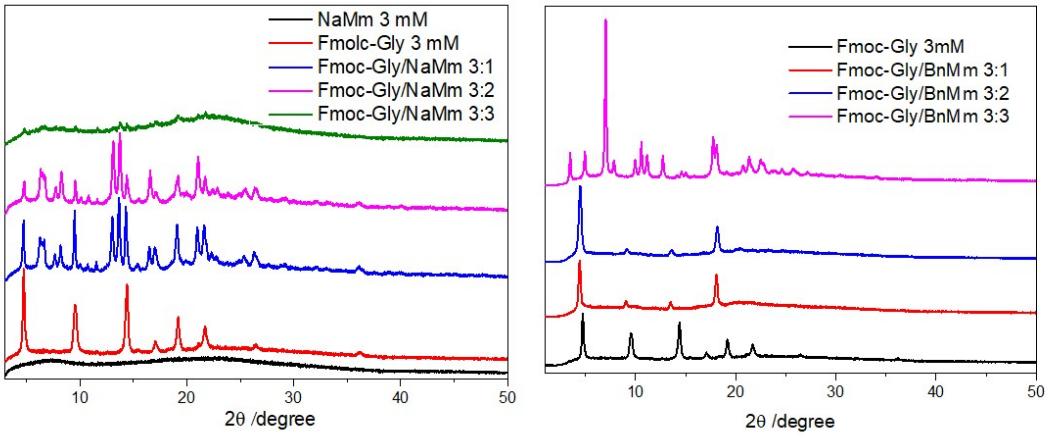

Figure S17 XRD patterns of co-assembled **Fmoc-Gly** and other melamine derivatives.

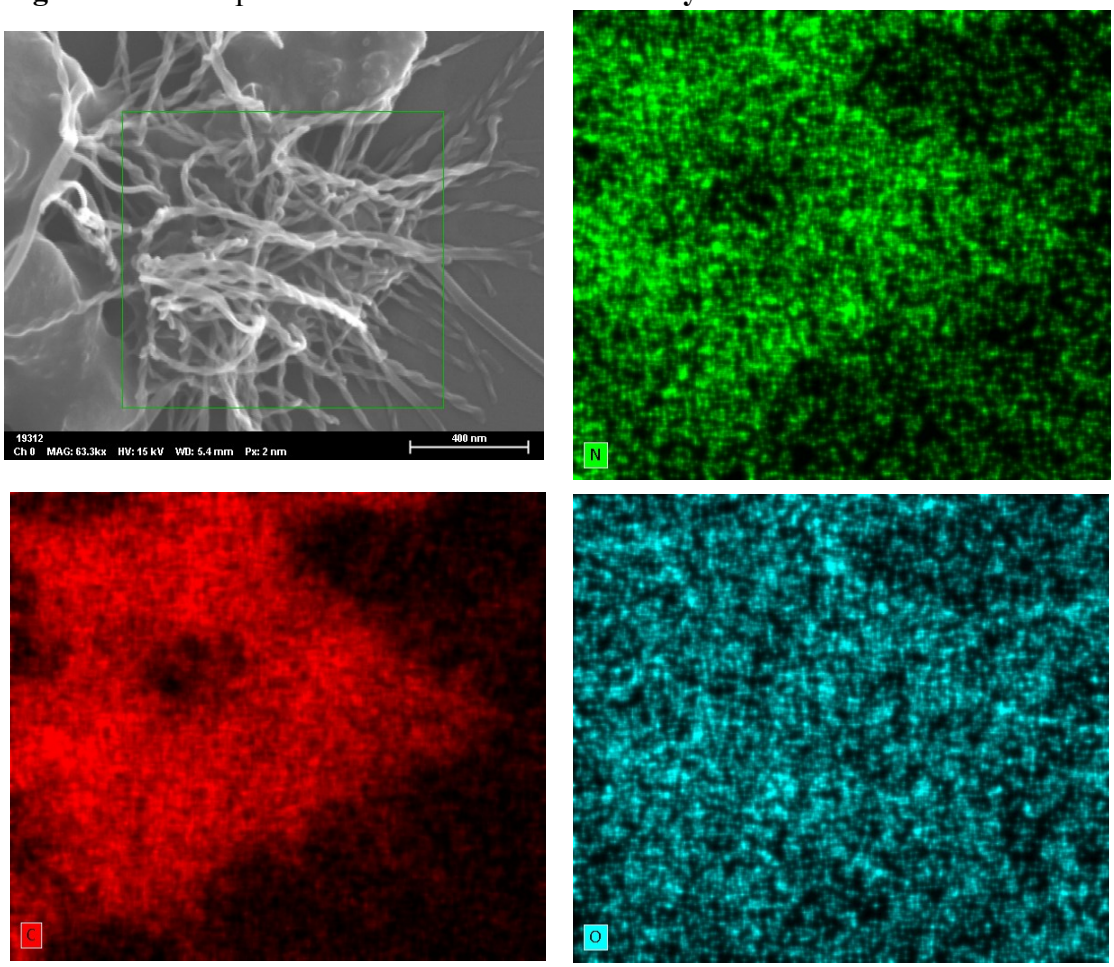

Figure S18. EDX element distribution of **Fmoc-Gly/BaMm** (3:2) double helical structures.

Table S1 Crystal data of **BaMm**.

Deposition Number	2072055
Formula	C21 H18 N6
Temperature(K)	100
Wavelength	1.54184Å

Crystal system	triclinic
Space group	P 1
a, b, c/Å	a 11.7863(14) b 24.768(3) c 28.259(3)
V, Å3	7211.59
Cell angles	α 112.963(3) β 96.270(3) γ 103.206(3)
Z, Z'	Z: 16 Z': 0
R-factor (%)	15.06

Table S2 Crystal data of **NaMm**.

Deposition Number	2072054
Formula	C33 H24 N6
Temperature(K)	293
Wavelength	1.54184**Å**
Crystal system	monoclinic
Space group	P 21/n
a, b, c/Å	a 15.2765(7) b 7.2467(3) c 24.6245(12)
V, Å3	2725.55
Cell angles	α 90 β 91.077(4) γ 90
Z, Z'	Z: 4 Z': 0
R-factor (%)	5.38

Reference

[1] Grossmann, T. N.; Seitz, O. Nucleic Acid Templated Reactions: Consequences of Probe Reactivity and Readout Strategy for Amplified Signaling and Sequence Selectivity. *Chem. Eur. J.* **2009**, *15*, 6723–6730.

[2] a) Xing, P.; Li, Y.; Xue, S.; Phua, S. Z. F.; Ding, C.; Chen, H.; Zhao, Y. Occurrence of Chiral Nanostructures Induced by Multiple Hydrogen Bonds. *J. Am. Chem. Soc.* **2019**, *141*, 9946−9954; b) Aryaa, K.; Dandia, A. Synthesis and Cytotoxic Activity of Trisubstituted-1,3,5-Triazines. *Bioorg. Med. Chem. Lett.* **2007**, *17*, 3298–3304; c) Sha, Y.-W.; Dong, Y.-Y.; Han, T. Synthesis of 2,4,6-Tri(arylamino)-1,3,5-Triazine Derivatives and Microwave Irradiation Effect. *Youji Huaxue* **2003**, *23*, 380-383.